COBEM 2021 26th International Congress of Mechanical Engineering
ABCM Associação Brasileira de Engenharia e Ciências Mecânicas
November 22-26, 2021, Virtual Congress, Brazil

COB-2021-1031
LARGE-EDDY SIMULATION OF TURBULENT INCOMPRESSIBLE ROUND JET FLOW

Livia S. Freire
Instituto de Ciências Matemáticas e de Computação, University of São Paulo, São Carlos, Brazil
liviafreire@usp.br

Abstract. *The axisymmetric turbulent jet flow is one of the classical fluid dynamics problems that contributes significantly to the theory of turbulence, in addition to being part of relevant applications in engineering and industry. In this study, we use Large-Eddy Simulation (LES) to simulate a jet flow with Reynolds number $Re_D = 2.8 \times 10^4$ with an affordable computational cost. The results obtained are satisfactory, with a self-similar region that matches the established theory of jet flows. Results can likely be improved by increasing the domain size and resolution near the inlet. Regarding the dynamic Smagorinsky subgrid-scale model of the LES, we test the hypothesis that the Smagorisky coefficient should be scale-dependent for this type of flow, by comparing the results of the scale-invariant case with the simulation using a scale-dependent coefficient. Although in previous simulations of channel flow the scale-invariant model was underdissipative, which was improved by the scale-dependent model, in the jet flow the scale-invariant model already provided satisfactory results, and they became overdissipative when the scale-dependent model was used. Future work should deepen the investigation in order to identify the cause of this deterioration.*

Keywords: *jet flow, large-eddy simulation, dynamic Smagorinsky model.*

1. INTRODUCTION

The axisymmetric turbulent jet is one of the classical fluid dynamics problems that has been studied in details during the past century. It is a free shear flow, which implies that it is not directly impacted by walls, and that turbulence arises from the velocity difference between the jet and the fluid in which it is injected. Due to its simplified configuration, many theories of turbulence have been investigated and verified using jet flow (Pope, 2000), giving it an importance that goes beyond its specific applications. Furthermore, jet flow has many important uses in engineering and industry, and it can have different configurations, including nozzle shape, flow properties (velocity, temperature, density, etc.) in both jet and ambient fluids, the presence of chemicals, and many others. Therefore, the study of jet flows is an ongoing research area that has much to contribute to the theoretical and applied fluid dynamics fields.

Jet flows are typically studied using laboratory experiments or numerical simulations. In the latter, Direct Numerical Simulation (the numerical solution of the three-dimensional Navier-Stokes equation) provides the most accurate results regarding the turbulence in the flow, but it has a computational cost that increases rapidly with Reynolds number. For that reason, Large-Eddy Simulation (LES) is typically used to represent high-Reynolds number flows with an affordable cost. In LES, a filtered version of the three-dimensional Navier-Stokes equation is resolved in a grid coarser than the smallest scales of the flow, and the effect of these unresolved scales on the filtered flow is represented by a subgrid-scale (SGS) model. Different options of governing equations' formulation, numerical methods and SGS models are available, and several approaches have been tested for the jet flow in recent years (e.g. Suto *et al.*, 2004; Bogey and Bailly, 2006; Zhang *et al.*, 2011; Ghaisas *et al.*, 2015; Marek *et al.*, 2015).

In this study we test a new approach, which comprises the filtered Navier-Stokes equation in rotational form in a Cartesian grid with spectral method in the radial directions and centered finite-difference method in the axial direction. The classical dynamic Smagorinsky SGS model is used, in which the residual stress tensor (the unclosed term of the filtered Navier-Stokes equation) is parameterized as $-2\nu_t\widetilde{S}_{ij}$ from the eddy viscosity assumption ($\widetilde{S}_{ij}$ is the resolved strain-rate tensor), combined with the parameterization of the eddy viscosity ν_t based on the mixing-length approach, i.e., $\nu_t = l_s^2|\widetilde{S}|$, in which l_s is the mixing length and $|\widetilde{S}| = (2\widetilde{S}_{ij}\widetilde{S}_{ij})^{1/2}$. In this model, l_s is assumed to be proportional to the filter (grid) size Δ ($l_s = C_s\Delta$), and the proportionality coefficient C_s, known as the Smagorinsky coefficient, is the only undetermined parameter, which is obtained dynamically from the resolved scales of the flow (hence *dynamic* Smagorinsky model) by evaluating the model in a resolved scale $\alpha\Delta$, $\alpha > 1$. In this study, we test the hypothesis that, for the jet flow, C_s should be scale-dependent, i.e., that C_s at Δ is not necessarily equal to C_s at $\alpha\Delta$. More details are given in the next section.

2. METHODS

The LES code used in this study solves the filtered Navier-Stokes equation in rotational form to ensure conservation of mass and kinetic energy, in addition to the incompressibility assumption, which corresponds to (Bou-Zeid *et al.*, 2005)

$$\frac{\partial \widetilde{u}_i}{\partial x_i} = 0, \tag{1}$$

$$\frac{\partial \widetilde{u}_i}{\partial t} + \widetilde{u}_j \left(\frac{\partial \widetilde{u}_i}{\partial x_j} - \frac{\partial \widetilde{u}_j}{\partial x_i} \right) = - \frac{\partial \widetilde{p}}{\partial x_i} + \nu \frac{\partial^2 \widetilde{u}_i}{\partial x_j \partial x_j} - \frac{\partial \tau_{ij}^D}{\partial x_j}, \tag{2}$$

where the symbol $\{\widetilde{\ }\}$ implies a filtered (resolved) variable at the scale Δ, $\widetilde{u}_i$ and x_i are the resolved velocity and position vectors using index notation, t is time and ν is the fluid molecular kinematic viscosity. The SGS part of the LES is represented by the following relations:

$$\tau_{ij} \equiv \widetilde{u_i u_j} - \widetilde{u}_i \widetilde{u}_j, \qquad \tau_{ij}^D \equiv \tau_{ij} - \tau_{kk}\delta_{ij}/3 \approx -2(C_{s,\Delta}\Delta)^2 |\widetilde{S}| \widetilde{S}_{ij}, \tag{3}$$

in which $\widetilde{S}_{ij} = 0.5(\partial \widetilde{u}_i/\partial x_j + \partial \widetilde{u}_j/\partial x_i)$ is the resolved strain-rate tensor, τ_{ij} is the residual stress tensor and τ_{ij}^D is its anisotropic (deviatoric) part, which in this code is modeled through the use of the eddy viscosity and mixing length assumptions described before (right side of Eq. (3)). The modified kinematic pressure $\widetilde{p}$ incorporates the isotropic part ($\tau_{kk}\delta_{ij}/3$) of the residual stress tensor, and it is solved using a Poisson equation resulting from continuity (Eq. (1)). The Smagorinsky coefficient $C_{s,\Delta}$ is obtained dynamically by applying the SGS model at a second filtering scale $\alpha\Delta$, $\alpha > 1$, such that

$$T_{ij} \equiv \widehat{\widetilde{u_i u_j}} - \widehat{\widetilde{u}}_i \widehat{\widetilde{u}}_j, \qquad T_{ij}^D \equiv T_{ij} - T_{kk}\delta_{ij}/3 \approx -2(C_{s,\alpha\Delta}\alpha\Delta)^2 |\widehat{\widetilde{S}}| \widehat{\widetilde{S}}_{ij}, \tag{4}$$

$$L_{ij} \equiv T_{ij} - \widehat{\tau}_{ij} = \widehat{\widetilde{u}_i \widetilde{u}_j} - \widehat{\widetilde{u}}_i \widehat{\widetilde{u}}_j, \qquad L_{ij}^D \equiv L_{ij} - L_{kk}\delta_{ij}/3 \approx C_{s,\Delta}^2 2\Delta^2 \left\{ \widehat{|\widetilde{S}|\widetilde{S}_{ij}} - \alpha^2 \beta |\widehat{\widetilde{S}}| \widehat{\widetilde{S}}_{ij} \right\}, \tag{5}$$

where the symbol $\{\widehat{\ }\}$ implies a variable filtered at the scale $\alpha\Delta$, and $\beta \equiv C_{s,\alpha\Delta}^2 / C_{s,\Delta}^2$ accounts for a possible scale dependency of the C_s parameter. The difference L_{ij} between the residual stress tensors at scales $\alpha\Delta$ and Δ, T_{ij} and $\widehat{\tau}_{ij}$ respectively (Eqs. (4) and (3)) can be calculated from both the resolved scales of the flow (Eq. (5) left side) and from the SGS model (Eq. (5) right side), and the error between these two estimates can be minimized by finding the best C_s value at each timestep of the simulation and location of the domain. In practice, this local approach of estimation leads to a highly variable value of C_s, making the simulation numerically unstable. For that reason, some averaging is typically used in order to stabilize the coefficient. In this study, given the inhomogeneous nature of the flow, an averaging in time along Lagrangian paths of fluid parcels is adopted, as described in more details by Bou-Zeid *et al.* (2005). Note that this averaging uses an exponential weighting function in the backward time integration, and therefore has a limited memory.

A relevant aspect of the dynamic Smagorinsky model is the assumption regarding the C_s behavior across scales of the flow. If it is assumed that it is scale-invariant, $C_{s,\Delta} = C_{s,\alpha\Delta}$ (i.e., $\beta = 1$) and the error can be minimized directly. This is a reasonable assumption if both Δ and $\alpha\Delta$ belong to the inertial range of the flow. However, if the filtering scales fall near the transition to the integral or dissipative scales, this assumption can be flawed. Examples of these situations are when the LES code is refined enough approaching the dissipative scales, in the regions of the flow close to walls, or when large-scale effects such as stratification, shear or rotation are present (Meneveau and Katz, 2000). In those cases, it may be important to adopt a value of $\beta \neq 1$, which can be either prescribed *a priori* or obtained dynamically from the resolved scales of the flow. In the latter, which is tested here, a third filtering is performed at the scale $\alpha^2\Delta$, and by reproducing the error estimation described above in between the scales $\alpha^2\Delta$ and Δ, a new equation is provided in order to obtain the scale dependency rate. Note that this dependency is assumed to be itself scale-invariant, by defining

$$\beta = \frac{C_{s,\alpha^2\Delta}^2}{C_{s,\alpha\Delta}^2} = \frac{C_{s,\alpha\Delta}^2}{C_{s,\Delta}^2}, \tag{6}$$

(see details in Porté-Agel *et al.* (2000); Bou-Zeid *et al.* (2005); Kleissl *et al.* (2006)).

In this study, two simulations were performed, one for the scale-invariant and another for the scale-dependent SGS models, using $\alpha = 2$. All simulation parameters were kept the same, and are listed in Tab. 1. The code solves the governing equations in a Cartesian grid, and in the two radial directions it uses a pseudo-spectral method combined with periodic boundary conditions. In the axial direction, a second-order accurate centered-differences scheme is used, requiring a staggered grid in which the axial velocity is defined at the top/bottom walls of the grid whereas the radial velocities and pressure are defined at the center of the grid. For time advancement, the fully explicit second-order accurate Adams-Bashforth scheme is used. At the outlet wall, zero axial gradients of the three velocity components are imposed. At the inlet, a top-hat velocity is imposed in the axial direction (constant/zero velocity in/outside the nozzle), which is set at the

bottom wall. The two radial velocities, on the other hand, are defined at a distance $\Delta z/2$ from the bottom wall, where we impose the theoretical equation for the mean radial velocity $\overline{u}(z = \Delta z/2, r)$ described below. Even though imposing a *mean* velocity in the instantaneous filtered velocity $\widetilde{u}(z = \Delta z/2, r)$ is not ideal, this is a common practice in wall-modeled LES (see Bou-Zeid *et al.* (2005) as an example) and we expect that it will not impact the results significantly, as it is close to zero and its value outside the nozzle should have a low impact on the flow overall.

Table 1. Large-Eddy Simulation parameters.

jet diameter, D [m]	4×10^{-3}
jet velocity, $\overline{w}_j$ [m s^{-1}]	7
fluid viscosity, ν [m^{2}s^{-1}]	1×10^{-6}
Reynolds number, $Re_D = \overline{w}_j D/\nu$	2.8×10^4
domain, $(L_x \times L_y \times L_z)D^{-1}$	$24 \times 24 \times 64$
number of grid points	$144 \times 144 \times 360$
grid spacing, $(\Delta x \times \Delta y \times \Delta z)D^{-1}$	$0.17 \times 0.17 \times 0.18$
timestep, Δt [s]	1.5×10^{-5}
Courant–Friedrichs–Lewy number	~ 0.3
number of timesteps	150 000
total simulation time, [s]	2.25

In order to interpret the results, we evaluate the mean flow properties according to the established theory of axisymmetric jet flows, in which the mean axial and radial velocities can be represented, respectively, by

$$f(\eta) = \overline{w}(\eta)/\overline{w}_0(\eta) = \exp(-A\eta^2), \tag{7}$$

$$h(\eta) = \overline{u}(\eta)/\overline{w}_0(\eta) = \eta \exp(-A\eta^2) - \frac{1 - \exp(-A\eta^2)}{2A\eta}. \tag{8}$$

In these equations, $\eta = r/(z - z_0)$, r and z are the radial and axial positions, respectively, $\overline{w}(z, r)$ and $\overline{u}(z, r)$ are the mean axial and radial velocities, respectively, $\overline{w}_0(z)$ is the mean axial velocity at the centerline and $A = \log(2)/S^2$. The parameters z_0 and S characterize the spread of the jet along the axial direction. By defining the jet's half-width $r_{1/2}(z)$ such that $\overline{w}(r_{1/2}(z), z) = \overline{w}_0(z)/2$, it is observed that the jet's half-width should increase linearly with axial position as $r_{1/2}(z) = S(z - z_0)$, $S \sim 0.1$. Furthermore, the mean axial velocity at the centerline can be described as $\overline{w}_j/\overline{w}_0(z) = (z/D - z_0/D)/B$, in which $\overline{w}_j$ and D are the jet nozzle velocity and diameter, respectively, with $B \sim 6$. From these relationships it is possible to evaluate the quality of the LES results and the impact of the scale dependency hypothesis.

3. RESULTS

Figures 1 and 2 show radial snapshots of the axial velocity field and axial snapshots of the vorticity field, respectively, obtained in the last timestep of the simulation, which gives an overall idea of the behavior of the jet. The main difference between the scale-invariant and scale-dependent simulations is a suppression of small resolved scales in the latter compared to the former (Fig. 2). Although near steady-state conditions were obtained in the last 50 000 timesteps, it is likely that in the upper half of the domain the development of the jet is being directly impacted by the boundary conditions. Therefore, we concentrate our evaluation in the lower part of the domain, and note that future studies should increase the domain size.

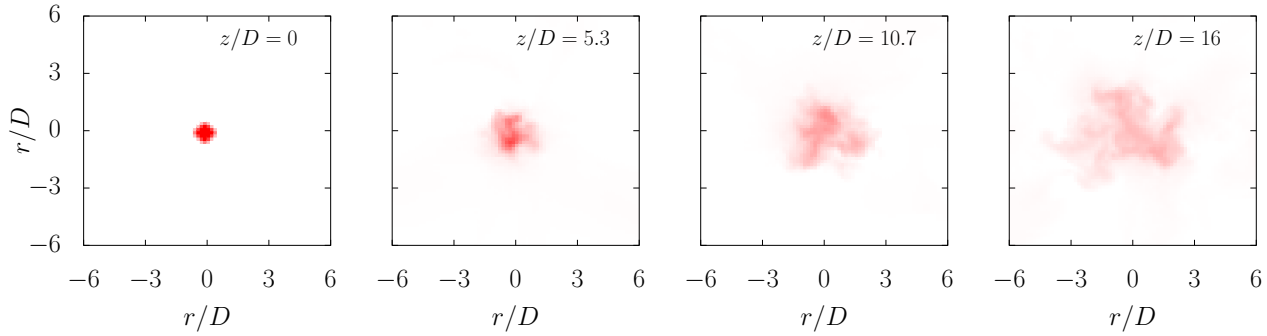

Figure 1. Snapshot of axial velocity in different axial planes in the last simulation timestep, for the scale-invariant simulation.

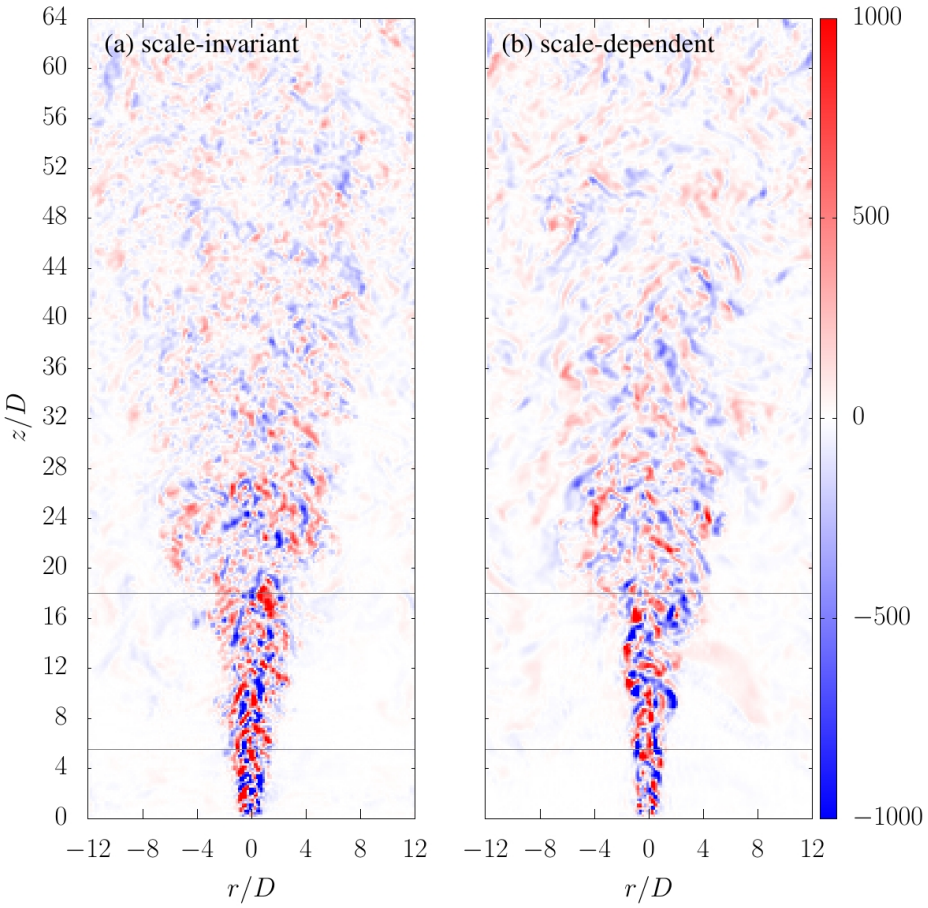

Figure 2. Snapshot of vorticity in the plane $y = L_y/2$ in the last simulation timestep, for the (a) scale-invariant and (b) scale-dependent simulations. Horizontal lines indicate the domain interval presented in Figs. 4 and 5.

Figure 3(a) presents the radial profiles of the mean axial velocity at different axial positions, for both simulations, showing that in the scale-dependent case there is a slightly faster jet near the nozzle. Although both simulations present a near-linear increase with z for the centerline velocity (Fig. 3(b)) and jet's half-width (Fig. 3(c)) as expected from the theory, they are better defined in the scale-invariant case. For that reason, we used the scale-invariant estimation of $z_0 = -0.67$ and $S = 0.1$ for all nondimensionalizations presented next. Note that the value of $B = 4.92$ obtained is lower than expected, but still in the correct order of magnitude. Furthermore, the negative value of z_0 is also unexpected, indicating that there is no transition region of initial development of the jet within the domain. If needed, this is something that can likely be improved in the future by using a refined grid near the wall and improving the lower boundary condition.

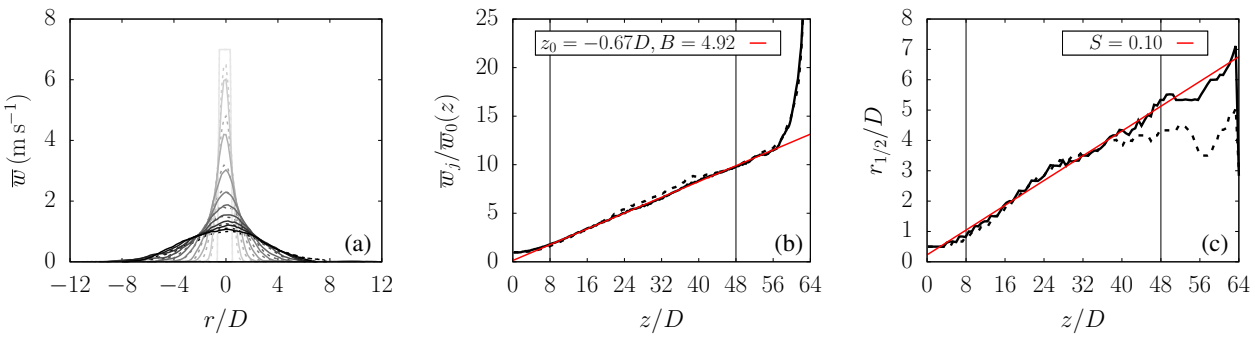

Figure 3. (a) Radial profiles of the mean axial velocity $\overline{w}$ from 1 to 10 Δz (from light to dark gray); (b) inverse of the mean axial velocity at the centerline $\overline{w}_j/\overline{w}_0(z)$ as a function of the axial distance z/D; (c) jet's half-width $r_{1/2}$ as a function of the axial distance. Red lines are the best linear fits within the interval defined by the vertical lines. Results from scale-invariant (solid) and scale-dependent (dashed) simulations.

The mean axial and radial velocities show the self-similar behavior predicted in the theory (Fig. 4), although it is better defined for the axial than the radial velocity. For the scale-dependent simulation, this self-similar behavior is reached further forward in the domain, whereas in the scale-invariant case the mean radial velocity is more disturbed at $18D$, possibly by the boundary conditions. In the case of the second-order statistics (Fig. 5), the self-similar behavior is not reached until much further forward in the domain, also indicating that a larger domain should be simulated in order to obtain a more appropriate and longer self-similar region. In comparison with experimental data, these statistics reach the correct value in the scale-invariant case, and surpasses them in the scale-dependent case, another indication of the superiority of the scale-invariant simulation.

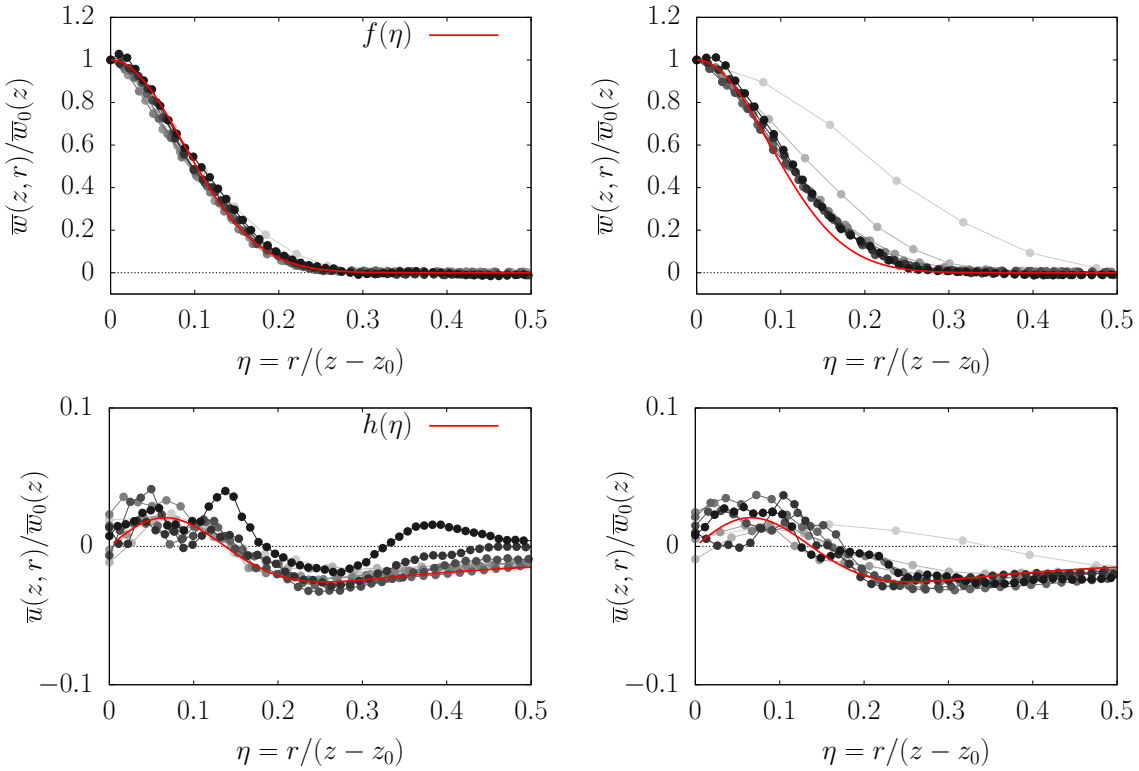

Figure 4. Self-similar radial profiles of mean axial (top) and mean radial (bottom) velocities, from the scale-invariant (left) and scale-dependent (right) simulations. Increasing axial distance from 5.5 to $18D$ (light to dark gray). The theoretical models $f(\eta)$ and $h(\eta)$ (Eqs. (7) and (8)) are shown in red.

In order to further investigate the differences between the two simulations, Fig. 6 shows the mean value of the eddy viscosity ν_t obtained for each simulation. As expected, higher values are obtained in the turbulent region, and $\nu_t \to 0$ in the laminar regions of the flow (McIlwain and Pollard, 2002). Furthermore, in the white regions of the figure (mostly located outside the jet), the value of ν_t is as low or smaller than the molecular viscosity $\nu = 10^{-6}\,\mathrm{m^2 s^{-1}}$ (which becomes the dominant viscosity parameter). Overall, higher ν_t values were obtained in the scale-dependent simulation, which explains the suppression of small resolved scales observed in Fig. 2. This is caused by values of $\beta < 1$ (note that $C_{s,\Delta} = C_{s,2\Delta}/\beta^{1/2}$ and $\nu_t \sim C_{s,\Delta}$), which was also obtained in the channel flow simulations of Bou-Zeid *et al.* (2005) and Kleissl *et al.* (2006). In their cases, the scale-invariant approach was identified as underdissipative, and the increased eddy viscosity obtained in the scale-dependent simulations provided an appropriate solution. In this jet flow simulation, on the other hand, the scale-dependent results seem to be overdissipative, as it can be observed by the one-dimensional energy spectra presented in Fig. 7. Note that the scale-invariant results are closer to the expected $k_r^{-5/3}$ decay than the scale-dependent case, which has a slightly steeper decay (especially in the radial velocity) and less energy near the inlet.

Overall, the scale-dependent model is expected to be more general than the scale-invariant one, especially in a flow with different levels of turbulence (and hence different scales) being filtered by the grid size Δ, such as the jet flow. However, the scale-dependent results presented here seem to deteriorate compared to the scale-invariant model. The exact reason for this behavior is difficult to identify, given the impact of the resolved flow on the SGS model and vice-versa (*which one is the primary cause?*). More specifically, it is difficult to predict the behavior of the SGS model (which is a function of $\widetilde{S}_{ij}$) compared to the behavior of the energy cascade through L_{ij} (*which term goes to zero faster, for example?*). Note that if all filtering scales (Δ, 2Δ and 4Δ) were within the inertial range, the value of β should be approximately 1 *on average*. On the jet flow, however, the turbulence is not homogeneous and part of the simulation has a non-turbulent flow, making it difficult to predict the relationship between all scales and the filter size Δ.

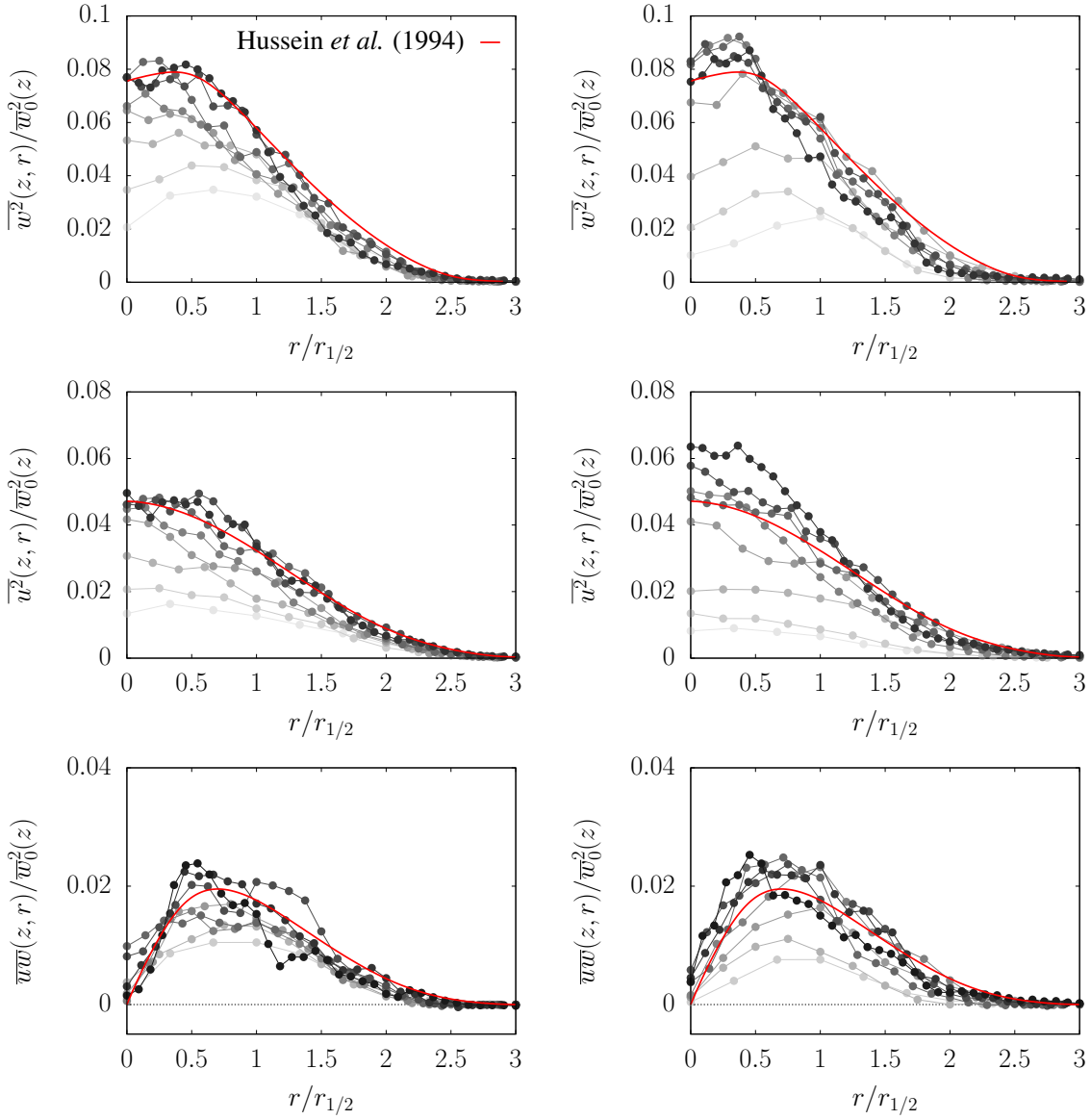

Figure 5. Self-similar radial profiles (as in Fig. 4) of Reynolds stresses (top: axial velocity variance; middle: radial velocity variance; bottom: shear stress). Results from scale-invariant (left) and scale-dependent (right) simulations. Red lines correspond to the experimental results with $Re_D = 9.5 \times 10^4$ from Hussein *et al.* (1994).

One possible cause of deterioration in the scale-dependent simulation is an increase in $C_{s,\Delta}$ (and consequently in ν_t) because $\beta \to 0$ due to $C_{s,4\Delta} \to 0$ while $C_{s,2\Delta}$ does not, since $\beta = C_{s,4\Delta}^2 / C_{s,2\Delta}^2$ (Bou-Zeid *et al.*, 2005), which can be caused by the second test filter scale 4Δ being at a scale even lower than the production scale. In other words, it is possible that the requirement of a third filtering scale is not appropriate for the level of turbulence (and size of the inertial range) of the flow being simulated here. In order to confirm this hypothesis, more investigation is needed, including a study of the behavior of the parameters $C_{s,\alpha\Delta}$ and β at different regions of the flow.

4. CONCLUSION

In this study, an LES of axissymetric jet flow with high Reynolds number was successfully performed, providing results that match the expected behavior from jet flow theory. The simulation was performed with an affordable cost in a personal computer, taking around three days for each simulation to run in parallel using 4 processors (the Intel Core i7 processor was used). If needed, results can likely be improved by increasing the domain size in order to extend the self-similar region of the flow, in addition to a grid refinement near the nozzle if a better transition region is needed.

Because the jet flow is inhomogeneous and have different scales being filtered by the grid size, it seemed likely that the SGS dynamic Smagorinsky model would require a scale-dependent coefficient. This hypothesis was tested here and it did not confirm the expectation. The satisfactory results obtained with a scale-invariant coefficient deteriorated when

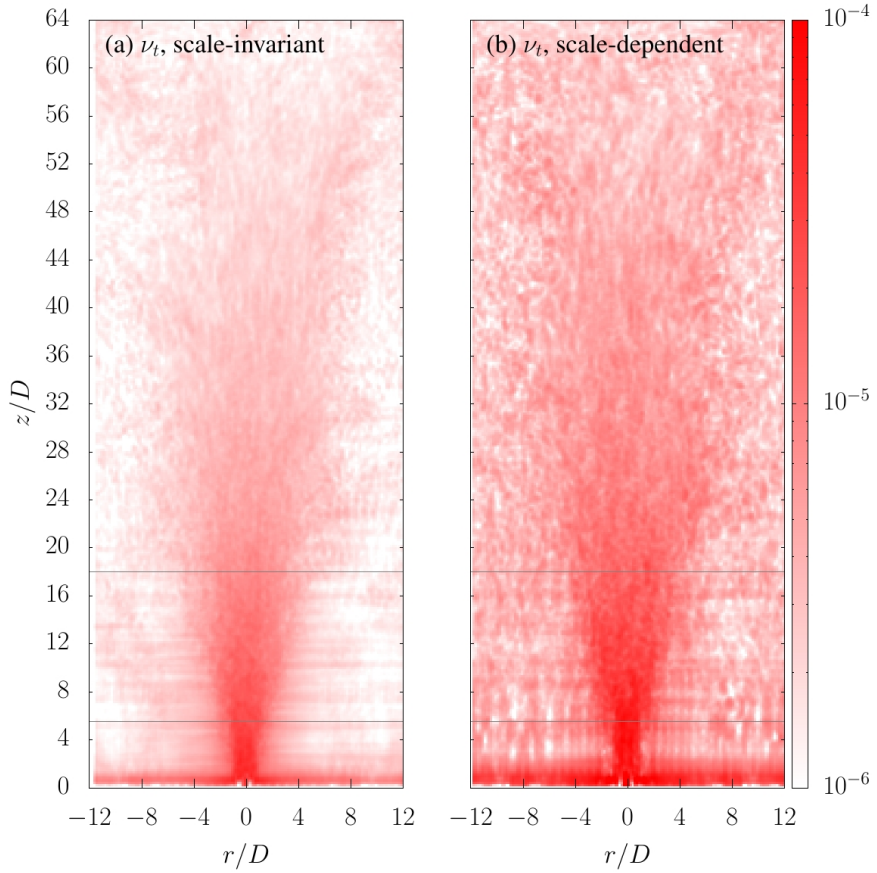

Figure 6. Mean value of the eddy viscosity ν_t in the plane $y = L_y/2$, for the (a) scale-invariant and (b) scale-dependent simulations. Horizontal lines indicate the domain interval presented in the next figure.

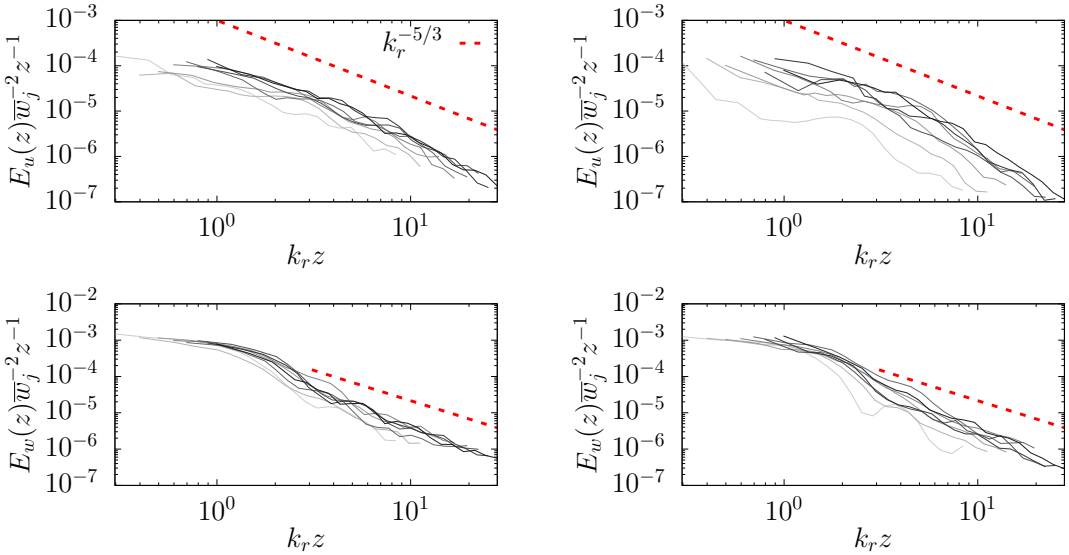

Figure 7. Normalized one-dimensional energy spectra in the radial direction, for different axial positions (from 5.5 to $18D$, light to dark gray), from the radial (top) and axial (bottom) velocities, and from the scale-invariant (left) and scale-dependent (right) simulations. Red lines correspond to the $k_r^{-5/3}$ decay rate.

the coefficient became scale-dependent, even though the latter is more general and should recover the scale-invariant result when applied in a "scale-invariant region of the flow" (a region of the flow where the scales Δ, 2Δ and 4Δ are within the inertial range). Therefore, it is likely that some assumption of the scale-dependent model is being violated, and more investigation is needed in order to identify the exact cause. The fact that the scale-invariant simulation is not

underdissipative is an indication that the scale-dependent model is not needed in this case, since the scale-dependent model was originally developed for these underdissipative cases (such as near the wall in channel flows).

Finally, we note that the jet flow is a useful flow configuration to test the limits of different SGS models under inhomogeneous conditions. As it changes from near-laminar to turbulence of variable intensity in space and time, it provides conditions to investigate in details the complex interaction between resolved and SGS flow features, which can be counterintuitive in many cases.

5. ACKNOWLEDGEMENTS

LF was funded by São Paulo Research Foundation (FAPESP, Brazil) Grant No. 2018/24284-1. We thank Gustavo Buscaglia, Mickaël Bourgoin, Romain Volk and Thomas Basset for insightful discussions. This study is part of a FAPESP-Université de Lyon collaboration project (Grant No. 2020/06273-2).

6. REFERENCES

Bogey, C. and Bailly, C., 2006. "Large eddy simulations of round free jets using explicit filtering with/without dynamic smagorinsky model". *International Journal of Heat and Fluid Flow*, Vol. 27, No. 4, pp. 603–610. ISSN 0142-727X. doi:10.1016/j.ijheatfluidflow.2006.02.008. URL https://doi.org/10.1016/j.ijheatfluidflow.2006.02.008.

Bou-Zeid, E., Meneveau, C. and Parlange, M., 2005. "A scale-dependent lagrangian dynamic model for large eddy simulation of complex turbulent flows". *Physics of Fluids*, Vol. 17, No. 2, 025105. doi:10.1063/1.1839152. URL http://dx.doi.org/10.1063/1.1839152.

Ghaisas, N.S., Shetty, D.A. and Frankel, S.H., 2015. "Large eddy simulation of turbulent horizontal buoyant jets". *Journal of Turbulence*, Vol. 16, No. 8, pp. 772–808. doi:10.1080/14685248.2015.1008007. URL https://doi.org/10.1080/14685248.2015.1008007.

Hussein, H.J., Capp, S.P. and George, W.K., 1994. "Velocity measurements in a high-reynolds-number, momentum-conserving, axisymmetric, turbulent jet". *Journal of Fluid Mechanics*, Vol. 258, p. 31–75. doi:10.1017/S002211209400323X. URL https://doi.org/10.1017/S002211209400323X.

Kleissl, J., Kumar, V., Meneveau, C. and Parlange, M.B., 2006. "Numerical study of dynamic smagorinsky models in large-eddy simulation of the atmospheric boundary layer: Validation in stable and unstable conditions". *Water Resources Research*, Vol. 42, No. 6, p. W06D09. ISSN 1944-7973. doi:10.1029/2005WR004685. URL http://dx.doi.org/10.1029/2005WR004685.

Marek, M., Tyliszczak, A. and Bogusławski, A., 2015. "Large eddy simulation of incompressible free round jet with discontinuous galerkin method". *International Journal for Numerical Methods in Fluids*, Vol. 79, No. 4, pp. 164–182. doi:10.1002/fld.4043. URL https://doi.org/10.1002/fld.4043.

McIlwain, S. and Pollard, A., 2002. "Large eddy simulation of the effects of mild swirl on the near field of a round free jet". *Physics of Fluids*, Vol. 14, No. 2, pp. 653–661. doi:10.1063/1.1430734. URL https://doi.org/10.1063/1.1430734.

Meneveau, C. and Katz, J., 2000. "Scale-invariance and turbulence models for large-eddy simulation". *Annual Review of Fluid Mechanics*, Vol. 32, No. 1, pp. 1–32. doi:10.1146/annurev.fluid.32.1.1. URL http://dx.doi.org/10.1146/annurev.fluid.32.1.1.

Pope, S.B., 2000. *Turbulent Flows*. Cambridge University Press.

Porté-Agel, F., Meneveau, C. and Parlange, M.B., 2000. "A scale-dependent dynamic model for large-eddy simulation: application to a neutral atmospheric boundary layer". *Journal of Fluid Mechanics*, Vol. 415, pp. 261–284. ISSN 1469-7645. doi:10.1017/S0022112000008776. URL http://dx.doi.org/10.1017/S0022112000008776.

Suto, H., Matsubara, K., Kobayashi, M. and Kaneko, Y., 2004. "Large eddy simulation of flow and scalar transport in a round jet". *Heat Transfer—Asian Research*, Vol. 33, No. 3, pp. 175–188. doi:https://doi.org/10.1002/htj.20001. URL https://doi.org/10.1002/htj.20001.

Zhang, H., Rong, Y., Wang, B. and Wang, X., 2011. "Large eddy simulation of a 3-d spatially developing turbulent round jet". *Science China Technological Sciences*, Vol. 54, No. 11, pp. 2916–2923. ISSN 1862-281X. doi:10.1007/s11431-011-4577-8. URL https://doi.org/10.1007/s11431-011-4577-8.

7. RESPONSIBILITY NOTICE

The author is solely responsible for the printed material included in this paper.